5 or even larger. We consider a case with the comparatively large core separation $D = 5$, to have negligible P_c/P_s. For $\rho = 3{\cdot}8\,\mu m$ and $\Delta = 0{\cdot}005$ (this gives $V \simeq 2{\cdot}4$ in the wavelength range of $1{\cdot}5$–$1{\cdot}6\,\mu m$), the coupling length will be about 16 cm. For nonlinear integrated optical waveguide couplers,

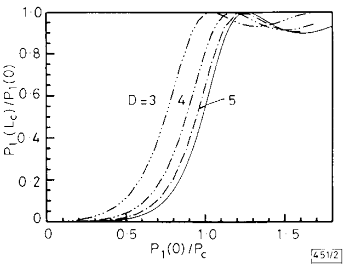

Fig. 2 *Nonlinear power transmission $P_1(z)/P_1(0)$ for $\pi/2$ (i.e. $\hat{C}_0\hat{Z} = C_0 z = \pi/2$) coupler for various values of D*

——— conventional result found by neglecting nonlinear mode field effect
Core separation $V = 2{\cdot}0$
Curves are labelled with D values

there is always a constraint on the device length due to the nature of the integration and the fabrication technique. It seems impractical to fabricate integrated waveguide couplers with lengths over 10 cm. Hence, nonlinear couplers will probably have to be made with small core separations, and thus nonlinear modal effects will have to be taken into consideration. This will be particularly relevant in cases where optical circuits using integrated optical waveguide couplers are to be designed with small dimensions for optical signal processing or computing.

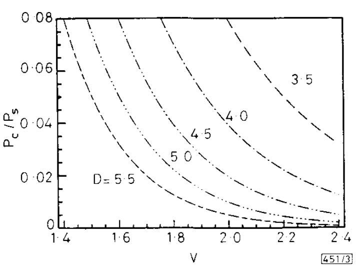

Fig. 3 *Ratio of critical power to single fibre selfguidance power P_c/P_s in optical switching using directional couplers*

In summary, we have examined the nonlinear mode field effects in nonlinear fibre couplers. We find that, even in cases where $P/P_s \ll 1$, the nonlinear change in the fundamental mode field in the cladding region can be quite significant. This implies that the nonlinear mode field effect can be an important factor in designing and analysing nonlinear optical devices, particularly those that depend on the evanescent part of optical guided waves.

Acknowledgment: A. Ankiewicz is grateful for the award of an Australian Research Council Senior Research Fellowship.

A. ANKIEWICZ
G.-D. PENG

30th July 1991

Optical Sciences Centre
Institute of Advanced Studies
The Australian National University
Canberra, ACT 2601, Australia

References

1 JENSEN, S. M.: 'Nonlinear coherent coupler', *IEEE J. Quantum Electron.*, 1982, **QE-18**, pp. 1580–1583
2 MENG, X. J., and OKAMOTO, N.: 'Improved coupled-mode theory for nonlinear directional couplers', *IEEE J. Quantum Electron.*, 1991, **QE-27**, pp. 1175–1181
3 ANKIEWICZ, A., and PENG, G. D.: 'Accurate variational method for nonlinear fibre devices', to be published in *Opt. Comm.*, 1991
4 PENG, G. D., and ANKIEWICZ, A.: 'Coupling of optical fibres determined by improved variational approximation', to be published in *J. Modern Optics*, 1991
5 CHIAO, R. Y., GARMIRE, E., and TOWNES, C. H.: 'Self-trapping optical beams', *Phys. Rev. Lett.*, 1964, **13**, pp. 479–482
6 SNYDER, A. W., and LOVE, J. D.: 'Optical waveguide theory' (Chapman & Hall, 1983)
7 SNYDER, A. W., and ANKIEWICZ, A.: 'Optical fiber couplers—optimum solution for unequal cores', *J. Lightwave Technol.*, 1988, **LT-6**, pp. 463–474
8 ANKIEWICZ, A.: 'Novel effects in non-linear coupling', *Opt. & Quantum Electron.*, 1988, **20**, pp. 329–337

SURFACE EMITTING SECOND HARMONIC GENERATION IN VERTICAL RESONATOR

Indexing terms: Resonators, Harmonic generation, Waveguides

The efficiency of surface emitting second harmonic generators can be significantly increased by resonating the second harmonic field in a vertical cavity structure. These resonant devices can be several orders of magnitude more efficient than similar nonresonant devices. Milliwatt visible outputs can be expected for tens of milliwatts of infra-red input in a doubly resonant structure for reasonable device parameters.

Introduction: Several workers[1,2] have demonstrated surface emitting second harmonic generation (SHG) in waveguide devices. The limited vertical interaction length reduces the efficiency of this interaction compared to collinear SHG. Even if quasi-phasematching methods[2] are used to solve the interference problem, the efficiency will increase with the core thickness only up to the point where the mode size begins to scale with the waveguide thickness. Although a waveguide resonator,[1] which increases the circulating pump power, is clearly an improvement over a nonresonant structure, the theoretical second harmonic power output for a realistic circulating pump power is still too low for many applications.

Resonating the second harmonic wave also increases conversion efficiency, as shown by Ashkin *et al.*[3] for the collinear case. The purpose of this Letter is to develop and apply a simply theoretical model for doubly resonant SHG with orthogonally propagating fundamental and second harmonic waves, as shown in Fig. 1.

Theory: Although it is possible to analyse this interaction exactly in the limit of no pump depletion by solving the appropriate boundary value problem,[4] a coupled cavity mode formalism[5] provides additional physical insight and allows treatment of pump depletion. For simplicity, we assume a slab waveguide geometry where both the fundamental and second

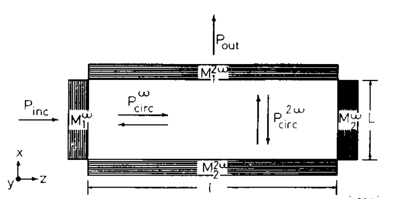

Fig. 1 *Side view of surface-emitting waveguide resonator geometry*

Coupling mirrors for pump and second harmonic field, respectively, are M_1^{ω} and $M_1^{2\omega}$, whereas nominal high reflectors are M_2^{ω} and $M_2^{2\omega}$, respectively harmonic fields are TE. In this case, we may write the electric field as

$$E_y = \tfrac{1}{2}\{a_1(t)N_1 f(x)\sin(\beta z)e^{-i\omega t} + ia_2(t)N_2\sin[k_{2\omega}(x+L/2)]e^{-i2\omega t} + \text{c.c.}\} \quad (1)$$

where $f(x)$ is the transverse field distribution, β is the propagation constant of the fundamental mode, and the dimensions of the waveguide resonator are $L \times w \times l$ (Fig. 1). The normalisation constants N_1 and N_2 are chosen such that the circulating powers are given by $P_{circ}^{\omega} = n_e L\omega |a_1|^2/n_\omega^2$, and $P_{circ}^{2\omega} = l\omega|a_2|^2/n_{2\omega}$, where the effective index of the fundamental mode is $n_e = \beta c/\omega$, and the indices of the core at ω and 2ω are n_ω and $n_{2\omega}$, respectively. The wavevector $k_{2\omega} = 2n_{2\omega}\omega/c$.

With this normalisation, the coupled equations for the on-resonance cavity mode amplitudes a_1 and a_2 are

$$\dot{a}_1 = -\kappa a_1^* a_2 - \gamma_1 a_1 + \varepsilon_i \quad (2)$$

$$\dot{a}_2 = \kappa a_1^2 - \gamma_2 a_2 \quad (3)$$

The interaction frequencies are assumed to be far enough from all material resonances that we can write the total nonlinear polarisation as $\mathscr{P}_{NL}(t) = 2\varepsilon_0 d_{eff} E^2(t)$ where d_{eff} accounts for the projection of the modal fields on the SHG tensor $\mathbf{d}$. We then find that the nonlinear coupling coefficient κ is real, due to the phase convention in eqn. 1, and is given by

$$\kappa = \frac{\sqrt{(8Z_0)}\omega d_{eff} I}{n_\omega^2 n_{2\omega}} \quad (4)$$

where Z_0 is the impedance of free space, and the dimensionless overlap integral I is

$$I = \frac{1}{L_e}\int_{-L/2}^{L/2} f^2(x)\sin[k_{2\omega}(x+L/2)]\,dx \quad (5)$$

where $L_e = \int_{-\infty}^{\infty} f^2(x)\,dx$ by definition. The linear loss parameters are

$$\gamma_1 = \frac{c}{2n_e l}[1 - \sqrt{(R_1^\omega R_2^\omega e^{-2\alpha_\omega l})}] \simeq \frac{c}{4n_e l}(T_1^\omega + \delta^\omega) \quad (6)$$

$$\gamma_2 = \frac{c}{2n_{2\omega}L}[1 - \sqrt{(R_1^{2\omega}R_2^{2\omega}e^{-2\alpha_{2\omega}\Lambda})}] \simeq \frac{c}{4n_{2\omega}L}(T_1^{2\omega} + \delta^{2\omega}) \quad (7)$$

and the driving term ε_i is

$$\varepsilon_i = \frac{c}{2n_e l}\left(\frac{n_\omega^2 T_1^\omega P_{inc}}{n_e \omega L}\right)^{1/2} \quad (8)$$

where P_{inc} is the incident power. All mirrors satisfy $R + T + A = 1$, where R is the reflectivity, T is the transmittance, and A is the loss of the mirror. The superscript and subscript notation for mirror quantities is shown on Fig. 1. The power attenuation coefficients for the fundamental and second harmonic modes are α_ω and $\alpha_{2\omega}$, respectively. Eqns. 2 and 3 correctly model the steady state behaviour for arbitrary input and output coupling, provided all other linear losses are small. If, in addition, the linear coupling is small, the simpler approximate forms for γ_1 and γ_2 given in eqns. 6 and 7 apply, where $\delta^\omega = T_2^\omega + A_1^\omega + A_2^\omega + 2\alpha_\omega l$, and $\delta^{2\omega} = T_2^{2\omega} + A_1^{2\omega} + A_2^{2\omega} + 2\alpha_{2\omega}L$.

The steady state form of eqns. 2 and 3 is

$$a_2 = (\kappa/\gamma_2)a_1^2 \quad (9)$$

and

$$a_1\left[1 + \frac{\kappa^2}{\gamma_1\gamma_2}|a_1|^2\right] = \frac{\varepsilon_i}{\gamma_1} \quad (10)$$

Because a_1 is in phase with ε_i, we lose no generality in taking ε_i to be real in eqn. 8. Eqn. 10 for real a_1 is a cubic with a unique solution.

In the low conversion limit, i.e. where $a_1 \simeq \varepsilon_i/\gamma_1$, we find, using eqns. 8, 9 and 10 and the relation $P_{out} = T_1^{2\omega}P_{circ}^{2\omega}$, that the surface-emitted second harmonic power P_{out} is

$$\frac{P_{out}}{P_{inc}^2} = \frac{128\pi^2 Z_0 d_{eff}^2 I^2}{n_e^2 n_{2\omega}\lambda_0^2}\frac{l}{\omega}\frac{4T_1^{2\omega}}{(T_1^{2\omega} + \delta^{2\omega})^2} \times \begin{cases} 1 & \text{single pass pump} \\ \left[\dfrac{4T_1^\omega}{(T_1^\omega + \delta^\omega)^2}\right]^2 & \text{resonant pump} \end{cases} \quad (11)$$

where λ_0 is the free space wavelength of the fundamental, and the low loss forms given in eqns. 6 and 7 are assumed to be valid. We see that the conversion efficiency in this limit is maximised by the usual low loss cavity impedance matching conditions for the resonant modes, namely $\hat{T}_1^{2\omega} = \delta^{2\omega}$ and, if the pump is resonant, $\hat{T}_1^\omega = \delta^\omega$, where $\hat{T}$ is the optimal coupling. If material losses are the dominant losses in the system, then $\delta^\omega \propto \alpha_\omega$, $\delta^{2\omega} \propto \alpha_{2\omega}$, and the dependence of the conversion efficiency of an optimally coupled device on the material parameters is of the form $d_{eff}^2/n_\omega^2 n_{2\omega}\alpha_\omega^2\alpha_{2\omega}$.

Discussion: Owing to their large absorption losses, III-V semiconductors with $2\hbar\omega$ greater than the direct bandgap, which have been used in conventional surface emitting second harmonic generators,[1] are clearly inappropriate for resonant second harmonic interactions. Nonlinear media with much lower absorption coefficients are better candidates for SHG of blue or green light, even if their nonlinear susceptibilities are somewhat smaller, e.g. wide-bandgap II-VI semiconductors. Certain organic crystals with very large nonlinear susceptibilities and moderate losses are particularly attractive for resonant applications. For example, 2-methyl-4-nitroaniline (MNA)[6] has an extremely large nonlinear susceptibility, $d_{11} = 250\,\text{pm/V}$, is relatively transparent at $0{\cdot}5\,\mu\text{m}$, and has already been grown in appropriate waveguide geometries.[7]

To calculate the efficiency of a resonant surface-emitting SHG device, we must evaluate the overlap integral I defined in eqn. 5. For simplicity, we analyse only the symmetric waveguide case, and assume the dielectric mirrors can be modelled as a uniaxial form-birefringent medium[8] at ω so that the cladding can be modelled with an index n_{cl} for TE modes. As the details of the cladding fields are unimportant here, this is an adequate approximation for ω when the mirrors are quarter wave stacks at 2ω. Finally, we assume the fundamental is propagating in the lowest-order transverse mode, so that

$$f(x) = \begin{cases} \cos(2U_x/L) & |x| \le L/2 \\ e^W \cos(U)e^{-W|2x/L|} & |x| \ge L/2 \end{cases} \quad (12)$$

Here the mode parameters U and W are given by $2U = k_0 L(n_\omega^2 - n_e^2)^{1/2}$, and $2W = k_0 L(n_e^2 - n_c^2)^{1/2}$, where $k_0 = \omega/c$. The eigenvalue equation for n_e is, from Reference 9, $W = U \tan U$. Owing to the simple form of $f(x)$, the overlap integral defined in eqn. 5 can easily be evaluated. Noting the cavity resonance condition for the second harmonic, $k_{2\omega}L = m\pi$, where m is an integer, we find

$$|I| = \frac{L}{L_e}\left|\frac{1}{m\pi} - \frac{m\pi\cos(2U)}{16U^2 - m^2\pi^2}\right| \quad (13)$$

for odd m and $I = 0$ for even m, where $L_e = \frac{1}{2}L(1 + 1/W)$ for this case. If quasi-phasematching were obtained by reversing the sign of the nonlinear coefficient every half wavelength, the overlap integral for odd m would be approximately m times larger.

The fundamental mode of an MNA waveguide with $\lambda_0 = 1{\cdot}06\,\mu\text{m}$, $n_\omega = 1{\cdot}8$, $n_{cl} = 1{\cdot}7$, $n_{2\omega} = 2{\cdot}2$, and $L = 3\pi/k_{2\omega} =$

$0{\cdot}36\,\mu$m has an effective index of $n_e = 1{\cdot}73$. If we further assume a nonresonant pump, $\omega = 5\,\mu$m, $l = 100\,\mu$m, $d_{eff} = d_{11} = 250$ pm/V, and $T_1^{2\omega} = \hat{T}_1^{2\omega} = \delta^{2\omega} = 0{\cdot}01$, and use eqn. 11 we find $P_{out}/P_{inc}^2 = 0{\cdot}05\,\text{W}^{-1}$. Because $m = 3$, we expect the efficiency to be approximately nine times larger if quasi-phasematching is employed (numerically we obtain a factor of 13·4), which gives $P_{out}/P_{inc}^2 = 0{\cdot}66\,\text{W}^{-1}$.

If both the pump and the second harmonic are resonant, the assumption of low conversion efficiency is no longer valid for an incident power of the order of 100 mW, as is easily seen from the above numerical result. In such cases, eqn. 11 is no longer valid, and the exact solution to eqns. 9 and 10 must be used. We give a numerical example here, reserving a more detailed analysis for future work. Assuming $A_1^{\omega} = A_1^{2\omega} = 0{\cdot}005$, $\delta^{\omega} = 0{\cdot}05$, no quasi-phasematching, and $P_{inc} = 100$ mW in addition to the above parameters, we find a maximum second harmonic power output of 36 mW for an optimal coupling given by $T_1^{\omega} = \hat{T}_1^{\omega} = 0{\cdot}097$, and $T_1^{2\omega} = \hat{T}_1^{2\omega} = 0{\cdot}027$. We see that high conversion efficiencies are possible for modest input power, and that the optimal coupling differs from that calculated in the low efficiency regime.

Conclusion: We have shown that vertical cavity resonant SHG structures can have significantly higher conversion efficiency than conventional surface emitting SHG devices, and have identified $d_{eff}^2/n_{\omega}^2 n_{2\omega}\alpha_{\omega}^2\alpha_{2\omega}$ as the relevant material figure of merit for a doubly resonant interaction. A phase-matchable nonlinearity is not necessary, as seen in the numerical example where tens of milliwatts of second harmonic were obtained for a 100 mW pump using the nonphase-matchable d_{11} coefficient of MNA. The efficiency may be significantly increased over that calculated here if quasi-phasematching techniques can be applied in this resonant geometry. Extension of this theory to TM modes, multilayer waveguides and interactions such as parametric amplification and oscillation will be given elsewhere.

Acknowledgments: This work is supported in part by DARPA, under contract number MDA972-90-C-0046, and R. Lodenkamper gratefully acknowledges the support provided by AT&T.

R. LODENKAMPER
M. M. FEJER*
J. S. HARRIS, JUN.

Solid State Laboratory
Stanford University
Stanford, CA 94305, USA

**Edward L. Ginzton Laboratory*
Stanford University
Stanford, CA 94305, USA

29th July 1991

References

1 VAKHSHOORI, D., WU, M. C., and WANG, S.: 'Surface-emitting second-harmonic generator for waveguide study', *Appl. Phys. Lett.*, 1988, **52**, (6), pp. 422–424
2 NORMANDIN, R., WILLIAMS, R. L., and CHATENOUD, F.: 'Enhanced surface emitting waveguides for visible, monolithic semiconductor laser sources', *Electron. Lett.*, 1990, **26**, (25), pp. 2088–2089
3 ASHKIN, A., BOYD, G. D., and DZIEDZIC, J. M.: 'Resonant optical second harmonic generation and mixing', *IEEE J. Quantum Electron.*, 1966, **QE-2**, (6), pp. 109–123
4 LIAO, C., BUNDMAN, P., and STEGEMAN, G. I.: 'Second harmonic generation with surface guided waves in signal processing geometries', *J. Appl. Phys.*, 1983, **54**, (11), pp. 6213–6217
5 ZIMMERMANN, C., KALLENBACH, R., and HÄNSCH, T. W.: 'Doubly-resonant second-harmonic generation in β-barium borate', *Opt. Commun.*, 1989, **71**, (3, 4), pp. 229–234
6 LEVINE, B. F., BETHEA, C. G., DRUMMOND, C. D., LYNCH, R. T., and BERNSTEIN, J. L.: 'An organic crystal with an exceptionally large optical second-harmonic coefficient: 2-methyl-4-nitroaniline', *J. Appl. Phys.*, 1979, **50**, (4), pp. 2523–2527
7 SASAKI, K., KINOSHITA, T., and KARASAWA, N.: 'Second harmonic generation of 2-methyl-4-nitroaniline by a neodymium : yttrium aluminum garnet laser with a tapered slab-type optical waveguide', *Appl. Phys. Lett.*, 1984, **45**, (4), pp. 333–334
8 YEH, P.: 'Optical waves in layered media' (Wiley, New York, 1988)
9 SNYDER, A. W., and LOVE, J. D.: 'Optical waveguide theory' (Chapman and Hall, London, 1983)

REVERSE HUFFMAN TREE FOR NONUNIFORM TRAFFIC PATTERN

Indexing terms: Codes and coding, Digital communication systems, Communication networks

The tree protocol has been an important protocol in multiaccess communication channels with traffic that arrives uniformly. In the Letter, a reverse Huffman tree protocol is proposed for multiaccess networks with nonuniform traffic pattern. Some tree construction protocols are developed and reverse Huffman tree protocol is shown to have the smallest delay.

Introduction: This Letter considers the multiple accessing of a broadcast channel by a set of independent stations. For broadcast channels, the resolution of channel contention is the heart of the multiaccessing problem, and the tree protocol provides a good solution.[1–4] However, the original tree protocol was designed for systems with uniform arrival rates.

In this Letter, a system with nonuniform arrival rates is considered. Because each station has its own traffic intensity which may be different from others, different structures may influence the average packet delay. The packet delay is a major issue of the system performance and is defined as the time from the instant that a packet arrives at a source to the instant that it is successfully received by its destination.

To build the tree for a system with nonuniform traffic pattern, we apply the coding schemes developed from coding theory to construct the tree. We notice that Huffman coding, the best coding scheme which minimises the average code length, has a good performance but does not achieve the best performance. Hence, we propose another scheme called the reverse Huffman code tree which achieves a better performance than the Huffman code tree.

Tree types and simulation results: We first propose four schemes in constructing the tree structure. We then run simulations to show and compare the performances of different schemes. To provide an example, we let $\vec{\lambda} = (1, 5, 6, 9, 12, 18, 23, 40)$. Note that the overall system arrival rate cannot exceed unity to achieve a stable system, hence this $\vec{\lambda}$ is just a scaled vector which shows the relative ratio of packet arrival rates to all stations.

(i) *Random:* In this method, we construct a balanced tree and randomly map stations to tree leaves.

(ii) *Low traffic first tree:* In this method, we build a balanced tree and map stations to tree leaves in an ascending order of the traffic arrival rates. Clearly, the delay performance of this tree will be poor and we will use it as the worst case in the performance comparison.

(iii) *Huffman code tree:* With one Huffman code method,[5] we can obtain a good tree structure and mapping. We arrange λ_i in a descending order and the depth d_i in an ascending order; i.e. we have both

$$\lambda_1 \le \lambda_2 \le \lambda_3 \le \ldots \le \lambda_N$$

and

$$d_1 \ge d_2 \ge d_3 \ge \ldots \ge d_N$$

Note that under this tree construction method, we minimise D over all structures where D is defined as $D = \sum_{i=1}^{N} \lambda_i d_i$. This D corresponds to the average code length in coding theory.

Algorithm:

(1) combine the two nodes with least transmission rates (j and k) into a dummy node; $\lambda_{dummy} = \lambda_j + \lambda_k$

(2) construct a binary tree; this dummy node is the father node, and the two corresponding nodes are descendants (left child and right child)

(3) delete λ_j and λ_k from $\vec{\lambda}$ and add λ_{dummy} to $\vec{\lambda}$; go to step 1